JOURNAL OF MAGNETIC RESONANCE **135,** 126–132 (1998)
ARTICLE NO. MN981551

Improved Hardware and Software for Single-Crystal NMR Spectroscopy

Thomas Vosegaard, Eigil Hald, Vagn Langer, Hans J. Skov, Preben Daugaard, Henrik Bildsøe, and Hans J. Jakobsen

Instrument Centre for Solid-State NMR Spectroscopy, Department of Chemistry, University of Aarhus, DK-8000 Aarhus C, Denmark

Received October 6, 1997; revised April 30, 1998

Design of state-of-the-art instrumentation and software for acquisition and analysis of single-crystal NMR spectra is presented. The design involves highly accurate rotation of a goniometer, and the acquisition of all the spectra for each rotation axis is automatically controlled by the host computer of the spectrometer using a home-built interface between the computer and the single-crystal probe. Moreover, a software package (*ASICS*) for fast and routine assignment/analysis of complex single-crystal spectra has been developed. Employing this equipment, the acquisition and complete analysis of single-crystal NMR spectra may be performed in about the same time as required for powder methods (spinning or static). The hardware and software are compared to recent alternative approaches within single-crystal NMR. Finally, it has been observed that single-crystal NMR techniques may provide the desired data for samples where powder methods fail.

INTRODUCTION

Single-crystal NMR spectroscopy is traditionally used for the determination of the magnitude and orientation (in the molecular/crystal frame) of the tensor for one or more of the anisotropic interactions encountered in solid-state NMR (e.g., chemical shielding anisotropy (CSA) (*1*), dipolar coupling (*2*), or quadrupole coupling (*3*)). However, single-crystal NMR is normally considered tedious, elaborate, experimentally sophisticated, and a method that usually requires large crystals in order to avoid excessively long spectrometer time. For these reasons, it has been of interest to develop new methods for determining the interaction parameters from polycrystalline powders particularly using spinning methods, e.g., magic-angle spinning (MAS). Although several techniques have been developed, the powder methods generally provide no (or only partial) information about the orientation of the tensorial interactions in the molecular frame. However, it has become possible to determine the relative orientation of two or more tensors describing these interactions from powder spectra.

Because of its high-resolution properties and insensitivity to intensity distortions caused by imperfect pulse excitation, single-crystal NMR has recently experienced a renaissance, for spin-$\frac{1}{2}$ as well as quadrupolar nuclei, in cases where powder methods fail. Such cases include (i) complex powder spectra resulting from overlap of patterns from many different sites (*4–8*), (ii) samples for which one of the interactions of interest is so weak that the effect of this interaction will be averaged by MAS even at low spinning frequencies (*6, 9*) or is hidden in the line broadening of the dominating anisotropic interaction when observed from static spectra of powder samples (*6, 7, 9–12*), and (iii) quadrupolar nuclei for which the quadrupole interaction is so strong that even the second-order broadening of the central transition is larger by more than an order of magnitude than the available spinning frequencies (*7, 8*).

For single-crystal NMR to be an attractive alternative to the powder methods the spectrometer time for acquiring the single-crystal spectra and the computational time for the data analysis must be comparable to those for powders. To accomplish these requirements several strategies have been undertaken for improving state-of-the-art single-crystal NMR. For example, the low sensitivity of the widely used three-face cube design (*13*) caused by a poor filling factor of the rf coil has been improved using a split-coil single-crystal probe in which the goniometer is placed outside the rf coil (*14*). A different approach to single-crystal NMR has been proposed by the Grant group (*15, 16*), who designed a single-crystal probe that uses 2D spectra to correlate two different crystal orientations. An improved probe using the same approach but with only six properly chosen crystal orientations has recently been presented (*17*).

We have recently introduced the design and construction of a new single-crystal NMR goniometer (*18*) based on the traditional three-axis rotation scheme. In this design the crystal is mounted on a dovetail-shaped tenon which fits into three mortises of the goniometer. This design not only gives an improved accuracy for the angle setting in the rotation of the crystal but also allows for a better filling factor than the three-face cube design. In addition, when XRD experiments are performed the background scattering usually caused by the material (e.g., Al_2O_3) of the latter cube design is eliminated by the new goniometer design. In this work we present our continued efforts to improve single-crystal NMR. This involves (i) the construction of a computer interface between the spectrometer and the single-crystal probe which provides fully automated rotation of the goniometer/crystal and acquisition of data for each rotation axis and (ii) a software package which in a

1090-7807/98 $25.00

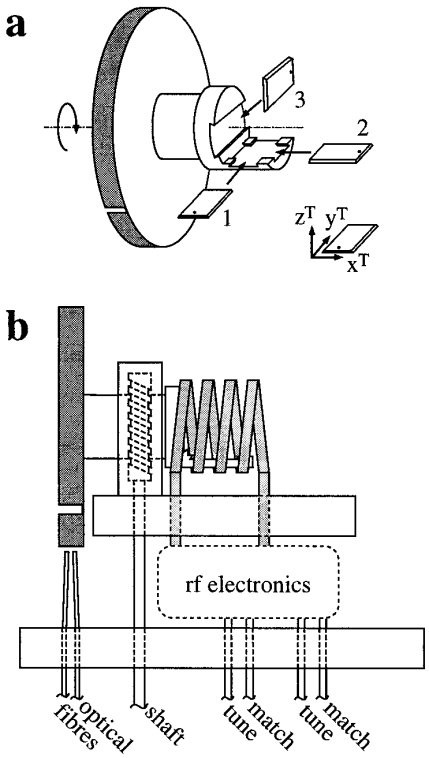

FIG. 1. Single-crystal NMR goniometer (*18*) showing the three dovetail mortises and a black cylinder with a narrow white mark for the reference point. (a) The tenon with the crystal glued onto its surface can be mounted in the three mortises marked 1, 2, and 3, thereby resulting in rotation about the $-x^T$ (1), y^T (2), and $-z^T$ (3) axis of the tenon frame, respectively. (b) The goniometer is enclosed by the double-tuned rf coil and with the rf electronics below. The optical fibers pointing at the black cylinder are used to locate the reference point for the rotation of the goniometer.

fast, simple, and semiautomated manner allows assignment and analysis of the resonances from even very complex single-crystal NMR spectra.

RESULTS

Hardware

Figure 1 shows the single-crystal NMR goniometer used in this work and recently described elsewhere (*18*). The crystal is glued (with an arbitrary orientation) onto a dovetail-shaped tenon which fits into the three mortises (marked 1, 2, and 3) of the goniometer and with the indicated axes of rotation (Fig. 1a), the three different mountings result in rotation about $-x^T$, y^T, and $-z^T$ of the tenon (T) frame. The rotation of the goniometer is perpendicular to the magnetic field and is performed using a worm gear combined with a vertical shaft that is operated from the bottom of the probe (Fig. 1b). Employing counterclockwise rotation in all operations of the vertical shaft results in an extremely high accuracy for the angular setting (*18*). The rotation of the vertical shaft is performed by a bipolar stepper motor (MAE—Motori ed Apparecchiature Elettriche, HY 200-2220-0100-AX 08) fastened onto a heavy brick of lead ($20 \times 20 \times 5$ cm^3, 23 kg) placed on the floor 70 cm below the bottom of an Oxford 9.4-T wide-bore magnet. The transmission between the probe and the stepper motor is a 40-cm-long shaft produced from POM (polyoxymethylene) with flexible aluminum couplings at each end and a universal coupling at the center. This makes the setup of the rigid single-crystal instrumentation simple, quick, and highly accurate. We note that the shaft must be produced from a nonconducting material to avoid pickup of noise in the spectra. The stepper motor has 200 steps per revolution and a reduction in the rotation of the goniometer of 1:20 is obtained by the worm gear (*18*). This results in a resolution of $360/(20 \times 200) = 0.09°$ for the rotation of the goniometer/crystal by each step of the stepper motor.

Although of improved accuracy for the crystal rotation, the present design, as is the case for other (published or commercial) single-crystal probes, still provides no reference point for the rotation of the crystal. This appears to be a general deficit in single-crystal NMR spectroscopy where the usual approach has been to take advantage of the relations between the three rotational axes (*5*) (*vide infra*). To improve on this shortage, a black 30-mm-o.d. cylinder, 4 mm high, with a narrow white mark on the outside of the cylinder is mounted on the horizontal shaft of the goniometer (Figs. 1a and 1b). Two optical fibers (one for transmission and the other for reflection of the emitted light) pointing at the black cylinder (Fig. 1b) are used to trigger the passage of the white mark and thereby the reference point for the crystal rotation. The accuracies for the rotation of the goniometer and for the reference point are measured by performing a 360° rotation of the goniometer starting from the reference point. Ideally this requires 4000 steps of the stepper motor, and we actually find that the reference point is reached within 4000 ± 1 steps, corresponding to the maximum obtainable accuracy of 0.09° for the angle setting of the goniometer/crystal.

The rotation angle of the goniometer (θ) is defined as the angle between the magnetic field and z^T, z^T, and x^T for the mountings 1, 2, and 3, respectively (Fig. 1a). Since NMR interactions are insensitive to rotation about the magnetic field axis, the spectra for the crystal orientations

$$\text{Mounting } 1(\theta = 0°) \equiv \text{Mounting } 2(\theta = 0°) \qquad [1]$$

$$\text{Mounting } 1(\theta = 90°) \equiv \text{Mounting } 3(\theta = 90°) \qquad [2]$$

$$\text{Mounting } 2(\theta = 90°) \equiv \text{Mounting } 3(\theta = 0°) \qquad [3]$$

will be pairwise identical. This is used to determine the zero point for the rotation ($\theta = 0$) and thereby the angle (θ_0) between the zero point and the reference point (provided by the white mark (Fig. 1)) for the rotation of the crystal/goniometer. For instance, using mountings 1 and 2 for acquisition of spectra by small rotation increments around the expected zero point ($z^T \| \mathbf{B}_0$) for the two rotation axes, the zero point is defined as

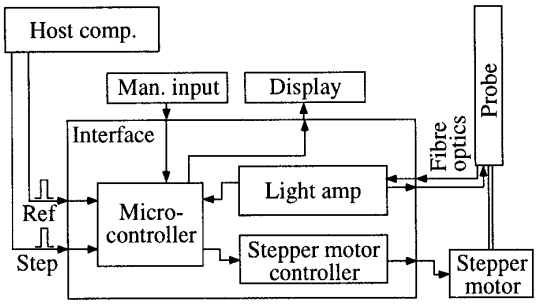

FIG. 2. Block diagram of the interface between the single-crystal probe and the host computer of the spectrometer. The heart of the interface is a microcontroller which takes two input signals from the host computer. The "Ref" pulse is used to locate the reference point of the rotation, while the "Step" pulse performs the stepwise rotation of the goniometer.

the point where the spectra for mountings 1 and 2 are identical (i.e., Eq. [1] is fulfilled). Using a properly chosen crystal (e.g., ^{23}Na in $NaNO_3$) this method provides a very accurate value for θ_0. An accuracy of $\pm 0.3°$ for θ_0 is obtained and determined by comparison of the values for θ_0 obtained independently from Eqs. [1]–[3]. It should be noted that the determination of θ_0 is a one-time measurement since its value does not change when the single-crystal probe is taken out of the magnet.

To obtain fully automated acquisition of all the spectra for each rotation axis, the stepper motor is interfaced to the spectrometer according to the block diagram shown in Fig. 2. The heart of the interface is a stepper motor controller (SGS-Thomson Microelectronics, GS-D200S) and a microcontroller (SGS-Thomson Microelectronics, ST62E25) which takes two input signals from the host computer of the spectrometer. One of the inputs (marked "Step") is used for the stepwise rotation of the goniometer; i.e., the stepper motor performs one step for each input pulse from the host. The other input (marked "Ref") is used to set the reference point for the rotation of the goniometer. Using this input the microcontroller automatically rotates the goniometer until it senses the reference point by the fiber optics. When the single-crystal probe is operated from the spectrometer, finding the zero point for the rotation is performed in two steps: (i) send a "Ref" signal and wait until the reference point has been found (it takes $\approx$40 s to perform a complete rotation of the goniometer and thus, this delay is set to 45 s) and (ii) send "Step" signals according to the determined value for θ_0 in order to set the zero point for the rotation. In this way, any pulse sequences may be used along with the single-crystal probe by adding a subroutine that controls the rotation supplied with values for θ and θ_0.

An example of the performance of the single-crystal instrumentation is given by the experimental 9.4-T ^{87}Rb single-crystal NMR spectra of Rb_2CrO_4 recorded using a crystal of size $2 \times 3 \times 4$ mm^3 and shown in Fig. 3, for rotation about the $-x^{\mathrm{T}}$ axis. For each rotation axis 21 spectra were recorded each following a 9° increment of the rotation angle. A spectral width of 500 kHz, single-pulse excitation ($\tau_p = 2\ \mu$s for $\gamma B_1/2\pi \approx$ 50 kHz), a relaxation delay of 2 s, and a total of 128 scans have been applied for each spectrum. Thereby, the total acquisition time for all 63 spectra of the three rotational axes was only 5 h. The complete analysis of these spectra is given elsewhere (*8*).

Software

In the high-field and secular approximations, the resonance frequency for a NMR interaction is given by (*19*)

$$\nu_{\lambda,m} = \langle m|\tilde{\mathcal{H}}_\lambda|m\rangle - \langle m-1|\tilde{\mathcal{H}}_\lambda|m-1\rangle, \qquad [4]$$

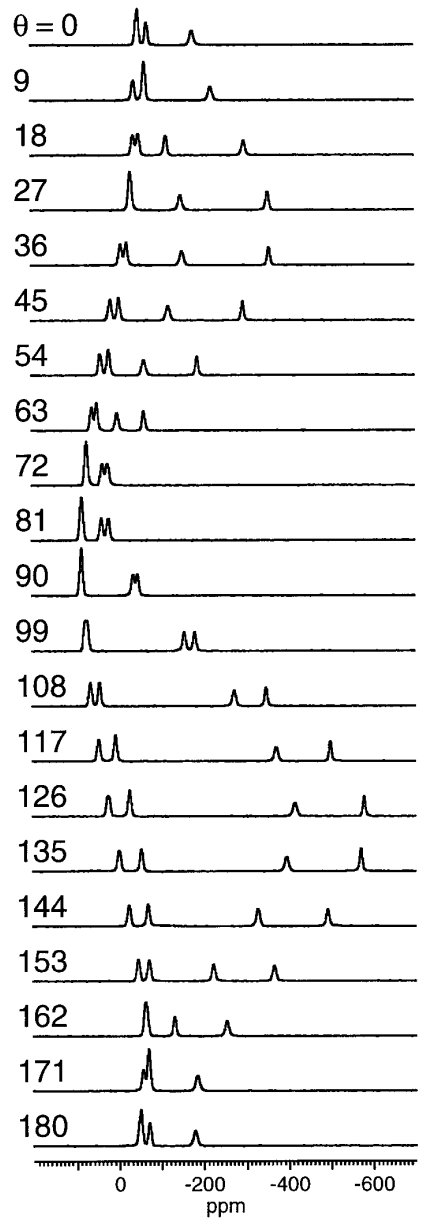

FIG. 3. Single-crystal ^{87}Rb NMR spectra of Rb_2CrO_4, each recorded following a 9° incrementation for the rotation about the $-x^{\mathrm{T}}$ axis.

where $m \leftrightarrow m - 1$ is the observed transition and $\lambda = Q$, σ, and D (quadrupole coupling, CSA, and heteronuclear dipole coupling) is the NMR interaction of interest. The Hamiltonian is usually dominated by the first-order term of its average Hamiltonian ($\tilde{\mathcal{H}}_\lambda \approx \bar{\bar{\mathcal{H}}}_\lambda^{(1)}$) given by

$$\bar{\bar{\mathcal{H}}}_\lambda^{(1)} = A_{0,0}^{\lambda,\mathrm{L}} T_{0,0}^{\lambda} + A_{2,0}^{\lambda,\mathrm{L}} T_{2,0}^{\lambda}, \qquad [5]$$

where $A_{j,m}^{\lambda,\mathrm{L}}$ are spatial irreducible tensor elements of the interaction tensor expressed in the laboratory (L) frame and $T_{j,m}^{\lambda}$ are the spin-tensor elements. The spatial tensor elements are readily calculated from the tensor expressed in the principal axis frame (P) by the coordinate transformations

$$\mathsf{A}^{\lambda,\mathrm{P}} \xrightarrow{\Omega_{\mathrm{PT}}^{\lambda}} \mathsf{A}^{\lambda,\mathrm{T}} \xrightarrow{\Omega_{\mathrm{TL}}^{\alpha}} \mathsf{A}^{\lambda,\mathrm{L}}, \qquad [6]$$

where $\Omega_{\mathrm{PT}}^{\lambda} = (\alpha_\lambda, \beta_\lambda, \gamma_\lambda)$ are the Euler angles describing the orientation of the (P) frame in the tenon/goniometer (T) frame, and $\Omega_{\mathrm{TL}}^{\alpha}$ are the Euler angles describing the transformation from (T) to (L) for a given rotation axis α ($= -x^{\mathrm{T}}, y^{\mathrm{T}}$, or $-z^{\mathrm{T}}$). Explicit expressions for $\mathsf{A}^{\lambda,\mathrm{P}}$ and T^{λ} are given elsewhere (*19*). Applying the coordinate transformations in Eq. [6] the resonance frequency for the Hamiltonian $\tilde{\mathcal{H}}_\lambda^{(1)}$ for each of the three rotational axes (α) is

$$\nu_{\lambda,\alpha}^{(1)}(\theta) = A_\alpha + B_\alpha \cos 2\theta + C_\alpha \sin 2\theta. \qquad [7]$$

In some cases the second-order term of the average Hamiltonian ($\tilde{\mathcal{H}}_\lambda^{(2)} = (1/2\nu_0)\ \{A_{2,2}^{\lambda,\mathrm{L}} A_{2,-2}^{\lambda,\mathrm{L}}\ [T_{2,2}^{\lambda}, T_{2,-2}^{\lambda}] + 2A_{2,1}^{\lambda,\mathrm{L}} A_{2,-1}^{\lambda,\mathrm{L}}\ [T_{2,1}^{\lambda}, T_{2,-1}^{\lambda}]\}$) must be included (e.g., for the central transition of quadrupolar nuclei possessing large quadrupolar interactions (*6–12, 20*)), which results in the following expression for the resonance frequency:

$$\nu_{\lambda,\alpha}^{(2)}(\theta) = A_\alpha + B_\alpha \cos 2\theta + C_\alpha \sin 2\theta + D_\alpha \cos 4\theta + E_\alpha \sin 4\theta. \qquad [8]$$

Explicit expressions for the coefficients of $\nu_{\mathrm{Q}}^{(1)}$, $\nu_{\mathrm{Q}}^{(2)}$, and $\nu_\sigma^{(1)}$ are given in Refs. (*6, 11, 18–20*).

The individual resonances at different rotation angles resulting from magnetically nonequivalent nuclei may be assigned using Eq. [7] or [8] depending on the interaction. To facilitate this assignment we have developed the software package *ASICS* (*A*nalysis of *S*ingle-*C*rystal *S*pectra). This makes use of a window on the screen of a workstation or the host computer which displays the resonance frequencies versus the rotation angle. The resonances are selected using the mouse, and the optimum curvature, given by Eq. [7] or [8], is calculated interactively. Thereby, a line corresponding to the optimum curve is drawn on the screen in order to help the assignment.

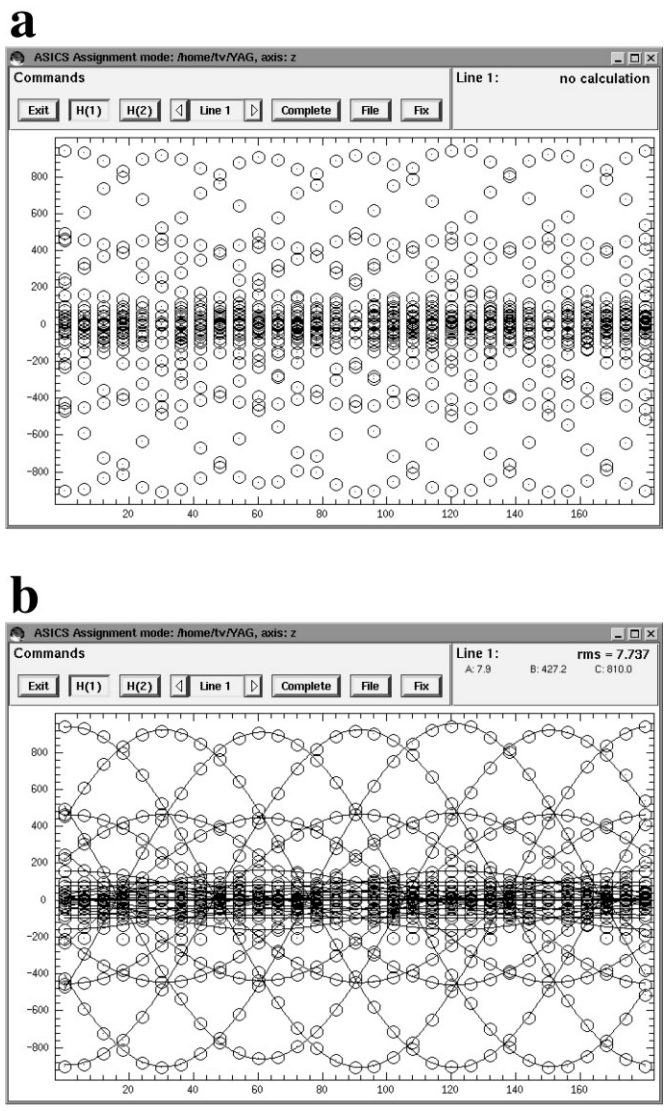

FIG. 4. Window on computer screen displaying the resonance frequencies versus the rotation angle and provided by the software package *ASICS*. (a) Unassigned ^{27}Al resonance frequencies for a garnet YAG ($Y_3Al_5O_{12}$) single crystal. A maximum of 35 resonance frequencies is observed for each rotation angle. (b) The complete assignment of the complex pattern in (a).

Figure 4a shows the screen provided for the ^{27}Al resonances from the ^{27}Al single-crystal NMR spectra of the garnet $Y_3Al_5O_{12}$ (YAG) for rotation about the $-z^{\mathrm{T}}$ axis. YAG has seven magnetically nonequivalent Al^{3+} sites in the unit cell (*21*) and with five observable ^{27}Al single-quantum transitions (spin $I = \frac{5}{2}$) a maximum of 35 resonance frequencies is expected in each spectrum. The complexity of the pattern of the resonances obviously complicates the assignment, but with *ASICS* we have found 32 resonance curves as shown in Fig. 4b. From the analysis (*24*) it turns out that four lines are overlapping for this rotation axis, and thus it has actually been possible to unravel the very complex pattern in Fig. 4a completely.

Following the assignment for the three rotation axes, it is

usually a straightforward matter to correlate the curves, resulting from the same magnetically equivalent nuclei, for each of the rotation axes by means of Eqs. [1]–[3]. This allows a determination of the relevant interaction parameters from the coefficients in Eqs. [7] and [8]. However, it is necessary to refine the parameters according to the minimum rms deviation

$$\mathrm{rms} = \left\{ \frac{1}{N} \sum_{i=1}^{N} (\nu_i^{\mathrm{e}} - \nu_i^{\mathrm{c}})^2 \right\}^{1/2} \qquad [9]$$

between the N experimental (ν_i^{e}) and calculated (ν_i^{c}) resonance frequencies for all three rotation axes. Thereby, a simultaneous fitting of (i) resonances from different transitions (e.g., satellite transitions for quadrupolar nuclei) and (ii) different crystallographically nonequivalent but magnetically equivalent nuclei (which have the same magnitudes and relative orientation for the interaction tensors), for the three rotational axes, is achieved.

For discussion of the quality of the parameters obtained and for comparison of the single-crystal method with other techniques it is important that the error limits be determined for each of the parameters. These error limits are estimated as 95% confidence intervals for the individual parameters (*25*), calculated from the χ^2 ($=\sum_{i=1}^{N} [(\nu_i^{\mathrm{e}} - \nu_i^{\mathrm{c}})/\sigma_i]^2$, σ_i is the measurement error for ν_i^{e}) function in a manner similar to that applied for the analysis of MAS spectra (*26*). Thus, the error limit $\delta(p)$ for a parameter p is calculated from the curvature of $\chi^2(p)$ obtained from optimizations employing fixed values of p near its optimum value. This curvature may be approximated by a second-order polynomial, and the 95% confidence interval is defined as $\delta(p) = 2/\sqrt{a}$, where a is the second-order coefficient of the polynomial (*25*). The optimizations and calculation of 95% confidence intervals are performed interactively by *ASICS*. A 95% confidence interval calculation typically requires 5–50 optimizations and uses 0.5–5 s of CPU time on a Sun SPARC 10/51 workstation.

In the analysis of the ^{87}Rb single-crystal NMR spectra of Rb_2CrO_4 (Fig. 3) it has been of particular interest to determine accurate parameters for the CSA interaction (δ_σ, η_σ) for the two Rb^+ sites (*8*). The CSA values (Rb(1): $\delta_\sigma = -80 \pm 7$ ppm, $\eta_\sigma = 0.19 \pm 0.14$; Rb(2): $\delta_\sigma = 109.7 \pm 0.6$ ppm, $\eta_\sigma = 0.037 \pm 0.010$ (*8*)) are determined with a very high accuracy. For demonstration of the goodness of these values, Fig. 5 shows plots of the minimum χ^2 value for different fixed δ_σ values for the rubidium sites 1 and 2 (Figs. 5a and 5b). This figure clearly displays well-defined minima for χ^2 for both sites, and the 95% confidence intervals are calculated from the optimum second-order polynomial shown with solid lines in Fig. 5. This example demonstrates the capability of the single-crystal technique for determination of CSA parameters in samples dominated by the quadrupole coupling where the powder

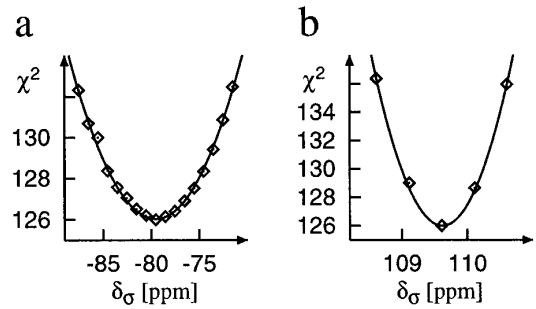

FIG. 5. Least-squares (χ^2) optimizations of δ_σ for the two Rb^+ sites in Rb_2CrO_4. The experimental points ($\diamond$) correspond to the minimum χ^2 value obtained for different fixed values of δ_σ for Rb sites 1 (a) and 2 (b). The solid lines represent the optimum second-order polynomial which is used to calculate the 95% confidence interval for δ_σ (Rb(1): $\delta_\sigma = -80 \pm 7$ ppm; Rb(2): $\delta_\sigma = 109.7 \pm 0.6$ ppm (*8*)).

(static and spinning) methods fail because of the strong quadrupole coupling interaction (*8*).

DISCUSSION

Several geometries for single-crystal NMR goniometers have been reported (*1, 13–18, 27–30*). The most common design uses a three- or four-faced cube that fits into the goniometer in three different ways, thereby resulting in rotation about three mutually perpendicular axes (*1, 13, 27, 28*). The crystal is fixed onto one of the faces of the cube and the design allows an easy repositioning of the crystal on the three rotation axes. However, when the cube–crystal setup is used for XRD studies the cube material (e.g., Al_2O_3) usually causes an unfavorable background scattering of the X rays. This problem is essentially eliminated in the present goniometer design since the crystal is covered only on one side by the tenon (*18*). Moreover, the dovetail joint between the tenon and goniometer gives an improved accuracy (0.3°) for the mounting of the crystal on the three axes as compared to the conventional cube design which has an accuracy of approximately 2° (*10, 13, 18*).

The low sensitivity that results from the poor filling factor of the cube design within the rf coil has been adressed by Hauser *et al.* (*14*). These authors presented a probe design with the intention to gain sensitivity while retaining a good compatibility between NMR and XRD experiments. In their design the crystal is mounted inside a small glass capillary and the goniometer is located outside a split rf coil. This design gives an improved sensitivity as demonstrated by the ^{31}P single-crystal NMR spectra of a 0.24-mm^3 HPA crystal (*14*). However, a direct comparison of the sensitivity resulting from the improved filling factor of the present goniometer design with that of the split-coil probe of Hauser *et al.* is not possible at this stage.

To facilitate the assignment of resonances for different rotation angles, Grant and co-workers (*15, 16*) have presented a modified version of the conventional three-rotation-axes de-

sign. This uses 2D correlation experiments to replace the conventional rotation plot studies. The worm gear of the traditional design is replaced by a string and a lever arm that allow a fast flip between two orientations of the crystal. Using this setup it is possible to obtain 2D spectra that correlate two crystal orientations. However, the flip-flop design still requires "manual" correlation between rotation curves from the three rotation axes. A more sophisticated probe design, also from the Grant group (*17*), has demonstrated that a full CSA-tensor study may be carried out by choosing only six different crystal orientations. With the proper equipment these six orientations may all be correlated by 2D flip-flop experiments (*17*). This design completely removes the problem of the assignment of resonances for different rotation angles and the correlation between different rotation axes. It is excellent for the measurement of chemical shielding tensors even from very complex single-crystal spectra (*17*). Furthermore, a 3D flip-flop-dipole experiment for the combined measurement of CSA and heteronuclear dipole tensors has been presented (*4*). However, since this design uses only six different crystal orientations, the method will generally fail when more than one NMR interaction is to be determined. For example, in the presence of the combined effect from quadrupole coupling and CSA the resonance frequency for the central transition of a quadrupolar nucleus depends on 11 parameters (C_Q, η_Q, δ_σ, η_σ, δ_{iso}, and the six Euler angles describing the orientation of the two tensors). Therefore, a minimum of 11 different crystal orientations is required in this case. Moreover, as demonstrated in Fig. 4, using the present software with a high-accuracy goniometer as described here (however, of traditional design), the assignment of even heavily overlapping rotation patterns can readily be performed. Most importantly, the hardware/software methodology described here for single-crystal studies does not depend on the number of interactions to be considered. The probe design of Grant and co-workers (*17*) therefore represents a completely different approach to single-crystal NMR than the present approach where the assignment is based on a semiautomated software (*ASICS*) analysis of high-accuracy experimental data. Whereas the present approach requires a careful computer analysis of the experimental data, the Grant procedure (*17*) generally results in a simpler analysis but requires longer spectrometer time because of the need for 2D spectra. Thus, the two methods appear complementary to one another, with respect to both the kind and number of interactions studied and the time spent either on the computer analysis or on the spectrometer.

CONCLUSION

Improved hardware and software for performing state-of-the-art single-crystal NMR are presented. The instrumentation includes a single-crystal NMR probe with a newly designed goniometer. The goniometer is rotated by a stepper motor controlled by the host computer of the spectrometer using a homebuilt interface. This instrumentation has made single-crystal NMR an attractive alternative to powder methods (spinning and static) with respect to the ease and accuracy for the data acquisition and the required spectrometer time. Combined with the software package *ASICS* the assignment and analysis of single-crystal NMR spectra become a fast and routine procedure even in the case of very complex spectra.

ACKNOWLEDGMENTS

The use of the facilities at the Instrument Centre for Solid-State NMR Spectroscopy, University of Aarhus, sponsored by Teknologistyrelsen, the Danish Research Councils (SNF and STVF), Carlsbergfondet, and Direktør Ib Henriksens Fond, is acknowledged. We thank Aarhus University Research Foundation for equipment grants.

REFERENCES

1. W. S. Veeman, *Prog. NMR Spectrosc.* **16,** 193 (1984).
2. H. van Willigen, R. G. Griffin, and R. A. Haberkorn, *J. Chem. Phys.* **67,** 5855 (1977).
3. R. V. Pound, *Phys. Rev.* **79,** 685 (1950).
4. M. H. Sherwood, D. W. Alderman, and D. M. Grant, *J. Magn. Reson. A* **104,** 132 (1993).
5. W. P. Power, S. Mooibroek, R. E. Wasylishen, and T. S. Cameron, *J. Phys. Chem.* **98,** 1552 (1994).
6. T. Vosegaard, J. Skibsted, H. Bildsøe, and H. J. Jakobsen, *J. Magn. Reson. A* **122,** 111 (1996).
7. T. Vosegaard, D. Massiot, N. Gautier, and H. J. Jakobsen, *Inorg. Chem.* **36,** 2446 (1997).
8. T. Vosegaard, I. P. Byriel, and H. J. Jakobsen, *J. Phys. Chem. B* **101,** 8955 (1997).
9. T. Vosegaard and H. J. Jakoben, *J. Magn. Reson.* **128,** 135 (1997).
10. K. Eichele, J. C. C. Chan, R. E. Wasylishen, and J. F. Britten, *J. Phys. Chem. A* **101,** 5423 (1997).
11. R. Blinc, J. Seliger, T. Apih, J. Dolinšek, I. Zupančič, O. Plyuschch, A. Fuith, W. Schranz, H. Warhanek, B. Topič, and U. Haeberlen, *Phys. Rev.* **43,** 569 (1990).
12. R. Blinc, J. Seliger, T. Apih, J. Dolinšek, A. Fuith, W. Schranz, and H. Warhanek, *Phys. Rev.* **52,** 833 (1995).
13. R. S. Honkonen, F. D. Doty, and P. D. Ellis, *J. Am. Chem. Soc.* **105,** 4163 (1983).
14. H. Hauser, C. Radloff, R. R. Ernst, S. Sundell, and I. Pascher, *J. Am. Chem. Soc.* **110,** 1054 (1988).
15. C. M. Carter, D. W. Alderman, and D. M. Grant, *J. Magn. Reson.* **65,** 183 (1985).
16. C. M. Carter, D. W. Alderman, and D. M. Grant, *J. Magn. Reson.* **73,** 114 (1987).
17. M. H. Sherwood, D. W. Alderman, and D. M. Grant, *J. Magn. Reson.* **84,** 466 (1989).
18. T. Vosegaard, V. Langer, P. Daugaard, E. Hald, H. Bildsøe, and H. J. Jakobsen, *Rev. Sci. Instrum.* **67,** 2130 (1996).
19. M. Mehring, "High Resolution NMR in Solids," Springer-Verlag, Berlin/Heidelberg (1983).
20. G. M. Volkoff, *Canad. J. Phys.* **31,** 820 (1953).
21. This has been deduced from the crystal structure of YAG (*22*) and the symmetry relations between the general positions (16(*a*)

and 24(*d*)) of the Al^{3+} ions (*23*) within the cubic space group $Ia\bar{3}d$.

22. F. Bertaud and F. Forrat, *C. R. Acad. Sci.* **242,** 382 (1956).

23. T. Hahn (Ed.), "International Tables for Crystallography," Vol. A, p. 706, Riedel, Dordrecht, Holland (1983).

24. T. Vosegaard, I. P. Byriel, D. A. Pawlak, K. Wozniak, and H. J. Jakobsen, *J. Am. Chem. Soc.* **120,** 7900 (1998).

25. W. H. Press, B. P. Flannery, S. A. Teukolsky, and W. T. Wetterling, "Numerical Recipes," Chap. 14.5, Cambridge Univ. Press, Cambridge (1989).

26. J. Skibsted, T. Vosegaard, H. Bildsøe, and H. J. Jakobsen, *J. Phys. Chem.* **100,** 14872 (1996).

27. A. Pines, J. J. Chang, and R. G. Griffin, *J. Chem. Phys.* **61,** 1021 (1974).

28. S. Pausak, J. Tegenfeldt, and J. S. Waugh, *J. Chem. Phys.* **61,** 1338 (1974).

29. S. Pausak, A. Pines, and J. S. Waugh, *J. Chem. Phys.* **59,** 591 (1973).

30. J. Kempf, H. W. Spiess, U. Haeberlen, and H. Zimmermann, *Chem. Phys.* **4,** 1338 (1974).